Journal of Molecular Structure, 273 (1992) 11–25
Elsevier Science Publishers B.V., Amsterdam

The high-resolution infrared spectrum of diacetylene and structures of diacetylene, triacetylene and dicyanoacetylene

D. McNaughton and D.N. Bruget

Department of Chemistry, Monash University, Wellington Road, Clayton, Victoria 3168 (Australia)

(Received 23 March 1992)

Abstract

The $\nu_6 + \nu_8$ combination band of diacetylene has been remeasured at 0.0019 cm^{-1} resolution with a Fourier transform infrared spectrometer. Analysis and assignment of the improved data sets were carried out with an interactive Loomis–Wood fitting program. Altogether more than 1400 assignments were made and band origins, rotational and distortion constants for the main band and associated hot bands were determined. The band centre was found to be 1241.060828(37) cm^{-1} and the ground-state rotational and distortion constants, B_0 and D_0, were found to be 0.14641021(52) cm^{-1} and 1.6085(49) $\times$ 10^{-8} cm^{-1}, respectively. The experimental values of B_0 for diacetylene, triacetylene and dicyanoacetylene are compared with values predicted from ab initio calculations, and with values obtained from estimates derived from the known structural parameters of HC_3N and HC_5N. Several very weak difference bands, $1_0^1 9_1^0$, $1_0^1 8_1^0$ and $4_0^1 6_1^0$, and combination bands, $5_0^1 6_0^1$ and $1_0^1 9_0^1$, in the region 3600–2600 cm^{-1} were also assigned.

INTRODUCTION

Diacetylene, H–C≡C–C≡C–H, the second member of the series of polyacetylenes $HC_{2n}H$ (n = 1,2,3 . . .) is known to exist in the interstellar medium and has been detected in the atmosphere of Titan [1,2]. It has been included as a minor species in ion molecule reaction schemes modelling the atmospheres of moons and planets such as Titan and Neptune [3]. Diacetylene is believed to have been formed on these planets from photochemical reactions of methane. The $6_0^1 8_0^1$ combination band of the symmetric (ν_6) plus antisymmetric (ν_8) C≡C–H bending modes of diacetylene is unusually intense due to the large change in dipole moment that occurs during the

Correspondence to: Dr. D. McNaughton, Department of Chemistry, Monash University, Wellington Road, Clayton, Victoria 3168, Australia.

bending vibrations. The $6_0^1 8_0^1$ band lies in the mid-infrared spectral region where there are few atmospheric absorptions, such that it provides a useful probe for interstellar detection of diacetylene by ground-based observations. Hardwick et al. [4] investigated the $6_0^1 8_0^1$ combination band at intermediate resolution (0.025 cm^{-1}) and obtained ground and excited state rotational and distortion constants for the main cold band. Their rotational assignments were later confirmed by Matsumura et al. [5] who investigated the $\nu_6 + \nu_8$ band by Stark modulation infrared diode laser spectroscopy. The other studies by infrared spectroscopy of diacetylene include the high-resolution analysis of the C – H (ν_4) and C≡C (ν_5) stretching modes by Guelachvili et al. [6]. We report here the generation of diacetylene by flash vacuum pyrolysis of 1,2,4,5-benzenetetracarboxylic dianhydride, and the analyses of the infrared spectra of the $6_0^1 8_0^1$ combination band measured at 0.0019 cm^{-1} resolution and of the weak $5_0^1 6_0^1$ and $1_0^1 9_0^1$ combination and $1_0^1 9_1^0$, $1_0^1 8_1^0$ and $4_0^1 6_1^0$ difference bands at 0.007 cm^{-1} resolution.

We also report here the results of ab initio calculations carried out in order to ascertain the molecular structures of diacetylene, triacetylene and, in particular, dicyanoacetylene where the available electron diffraction r_0 structure does not adequately predict the experimentally derived rotational constant.

EXPERIMENTAL

The experimental details have been described elsewhere [7] and Scheme 1 summarises the pyrolysis reaction. The precursor, 1,2,4,5-benzenetetracarboxylic dianhydride, was sublimed at 210°C and pumped into a 350 × 8 mm i.d. quartz tube heated to 1020°C (Scheme 1). Diacetylene and other pyrolysates such as CO, CO_2, C_2H_2 and C_6H_2 were deposited in a liquid nitrogen-cooled trap positioned at the exit of the furnace tube. Products more volatile than diacetylene were separated by warming the trap with successive applications of appropriate liquid nitrogen slush baths, and diacetylene was finally vaporised at −96°C into a multiple traversal infrared cell for the infrared measurements.

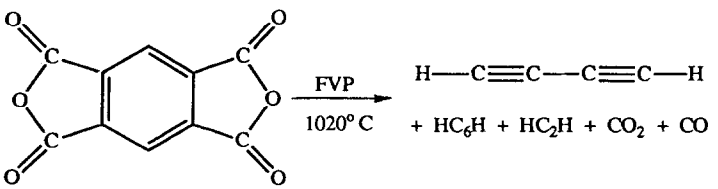

Scheme 1.

The gas-phase spectrum of diacetylene was measured under static conditions in the ranges 1380–980 cm^{-1} and 3950–1975 cm^{-1} using a Bruker HR 120 Fourier transform-infrared spectrometer equipped with liquid nit-

rogen-cooled MCT (1800–650 cm^{-1}) and InSb (4000–1800 cm^{-1}) detectors, and appropriate optical filters. The spectrum recorded at 0.0019 cm^{-1} resolution in the domain 1380–980 cm^{-1} consisted of 160 co-added scans, while the spectrum recorded at 0.007 cm^{-1} resolution in the range 3950–1975 cm^{-1} consisted of 420 co-added scans. The vapour pressures were maintained at 47 Pa and 133 Pa, respectively, and the path lengths were set to 18 m and 16 m. The spectra were calibrated by comparing positions of observed H_2O lines with those determined by Guelachvili and Rao [8]. The adjustment was -0.000532 cm^{-1} in the 1240 cm^{-1} region.

The spectra were analysed with the help of the interactive Loomis–Wood fitting program, MACLOOMIS [9], which enabled easy identification and rapid selection of the observed peaks. The ground and excited state rotational and distortion constants were determined by subjecting the observed line positions to a least-squares fit according to the expression

$$\tilde{\nu} = \tilde{\nu}_0 + (B'' + B')m - (B'' - D'' - B' + D')m^2 - (2D'' - H'' + 2D' - H')m^3 + (D'' - 3H'' - D' + 3H')m^4 + 3(H'' + H')m^5 - (H'' - H')m^6 \quad (1)$$

where $m = -J''$ and $J'' + 1$ for the P(J) and R(J) lines, respectively. The assignments were confirmed by calculating and fitting by least-squares the ground and excited state combination differences. For the degenerate Π vibrational states, the effective rotational constant has been expressed as $B_{av} = 1/2\ (B_{\Pi_e} + B_{\Pi_f})$ and the effective l-doubling constants as $q_v = B_{\Pi_f} - B_{\Pi_e}$ and $q_{vJ} = D_{\Pi_f}/D_{\Pi_e}$, where B_{Π_e}, B_{Π_f}, D_{Π_e} and D_{Π_f} have been determined separately. The vibration–rotation constants, α_i, have been calculated from the expression

$$B_v = B_e - \sum_i \alpha_i \left[v_i + \frac{d_i}{2} \right] \quad (2)$$

where v_i represents the set of vibrational quantum numbers and d_i is the degree of degeneracy of the ith vibrational mode.

Ab initio calculations were performed with the GAUSSIAN 88 suite of programs [10] on a VAX 6410 computer and on an IBM RISC 6000 540 computer. Geometry optimisations were carried out using the Hartree–Fock formalism at the 6-31G** level of theory and with electron correlation included at the MP2, MP3 and MP4 level with geometries constrained to linearity. Harmonic vibrational frequencies were computed at the optimised geometries. The optimised structural parameters and rotational constants of diacetylene, together with those for related long chain acetylenes and cyanoacetylenes, are presented in Table 1. Table 2 lists the scaled vibrational frequencies, intensities, normal modes of vibration and symmetry species for diacetylene.

TABLE 1

Bond lengths (pm) and rotational constants (cm^{-1}) of polyacetylenes and cyanopolyacetylenes[a]

Parameter	HF	MP2	MP3	MP4	Estimated	Experiment	El. Diff.
C_4N_2 (B_{exp} = 0.04458710(13) [11])							
$r_{C\equiv N}$	113.58	118.87	116.25	118.96	116.06[b]		116.1(5)[c]
$r_{C\equiv C}$	118.56	122.95	120.97	123.24	122.23[b]		119.8(11)[c]
r_{C-C}	138.94	136.89	138.53	137.85	136.36[b]		136.7(3)[c]
B	0.044951	0.04374	0.044108	0.043382	0.044611[b]		0.04489(9)[c]
C_4H_2 (B_{exp} = 0.14641021(52))							
r_{C-H}	105.71	106.22	106.14	106.49	105.8[d]		
$r_{C\equiv C}$	118.78	122.35	120.95	122.23	120.5[d]		
r_{C-C}	138.96	137.32	138.58	138.14	137.8[d]		
B	0.147790	0.144460	0.145205	0.143244	0.146521[d]		
C_6H_2 (B_{exp} = 0.04417223(15) [7])							
r_{C_1-H}	105.69	106.28	106.68	107.06	105.69[b]		
$r_{C_1\equiv C_2}$	118.83	122.60	120.99	122.91	120.87[b]		
$r_{C_2\equiv C_3}$	138.49	136.45	138.07	137.23	136.23[b]		
$r_{C_3\equiv C_4}$	119.14	123.40	121.43	123.71	122.23[b]		
B	0.044021	0.043557	0.043697	0.043196	0.044167		
HC_3N (B_{exp} = 0.15174022(1) [12])							
r_{C-H}	105.84	106.32	106.76	107.14		105.8[d]	
$r_{C\equiv C}$	118.52	122.2	120.74	122.48		120.5[d]	
r_{C-C}	139.09	137.51	138.76	138.36		137.8[d]	
$r_{C\equiv N}$	113.62	118.63	116.26	118.74		115.9[d]	
B	0.153620	0.148959	0.150424	0.147857		0.151812[d]	
HC_5N (B_{exp} = 0.0444084(1) [14])							
r_{C_1-H}	105.79	106.79	106.21	106.55		105.69	
$r_{C_1\equiv C_2}$	118.85	123.18	120.94	122.86		120.87	
$r_{C_2-C_3}$	138.77	136.37	137.99	137.22		136.23	
$r_{C_3\equiv C_4}$	118.71	122.50	121.22	123.53		122.23	
$r_{C_4-C_5}$	138.41	136.72	138.36	137.63		136.36	
$r_{C_5\equiv N}$	113.68	118.89	116.31	119.03		116.06	
B	0.044824	0.043744	0.043943	0.043322		0.044391	

[a]Theoretical calculations were carried out with 6-31G** basis sets assuming linearity.
[b]Estimated using the bond lengths of ref. 12.
[c]From ref. 13.
[d]From ref. 14.

TABLE 2

Observed and calculated vibrational wavenumber values, normal modes and symmetry species for diacetylene[a]

Species	Assignment	Vibration	Obs. Freq.[b]	Obs. Freq.[c]	HF/3-21G**	Intensity	HF/6-31G**	Int.
Σ_g^+	ν_1	C – H str.	3332.1541	3332.15476(35)	3291.33	0.00	3277.79	0.00
	ν_2	C≡C str.	2188.9285		2260.27	0.00	2253.36	0.00
	ν_3	C – C str.	871.9582		844.68	0.00	847.54	0.00
Σ_u^+	ν_4	C – H str.	3333.6647	3333.66465(20)	3289.44	172.43	3277.44	169.34
	ν_5	C≡C str.	2022.2415		2065.05	0.00	2074.14	0.10
Π_g	ν_6	H – C≡C bend	625.6436	625.49857(30)	740.71	0.00	724.29	0.00
	ν_7	C≡C – C bend	482.7078		478.58	0.00	550.19	0.00
Π_u	ν_8	H – C≡C bend	628.0409	627.89583(30)[d]	731.13	121.56	671.28	109.72
	ν_9	C≡C – C bend	220.1236	219.97784(44)	194.67	12.09	225.76	8.33

[a]The usual scaling factors of 0.9 and 0.8 have been applied to the stretching and bending modes, respectively.
[b]Guelachvili et al. [6].
[c]From $\nu_8 - \nu_6$ [15] and ν_4 (this work).
[d]This work.

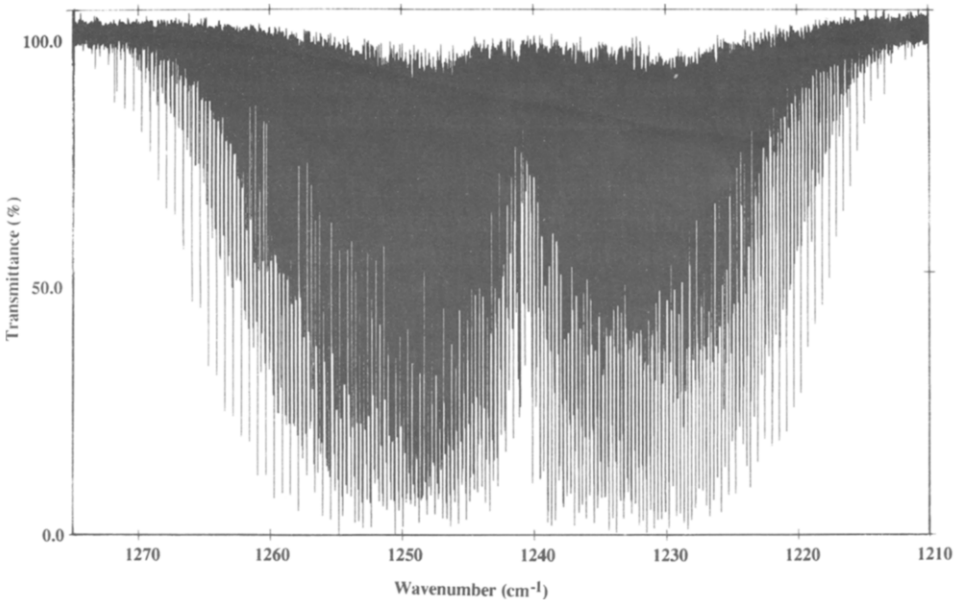

Fig. 1. The compressed high-resolution spectrum of the $6_0^1 8_0^1$ combination band of diacetylene.

RESULTS

The high-resolution gas-phase infrared spectrum of the $6_0^1 8_0^1$ combination band is reproduced in Fig. 1 and a screen-image of the Loomis–Wood diagram which presents the data in a more palatable format and includes sub-band assignments is depicted in Fig. 2. Altogether, sixteen sub-bands in addition to the main cold band have been identified and assigned. The 3 : 1 intensity alternation due to nuclear spin statistics for the rotational lines with different parity facilitated the J numbering and assignments for each series. The positioning of a central, unresolved, sharp Q-branch on the Loomis–Wood plot close to the band centre acted as a check for the J assignments of bands of the type Π–Π or Δ–Δ. The lower state rotational and distortion constants, B'' and D'', and vibration–rotation parameters, α_v, q_v'' and q_{vJ}'', for the cold band and various associated hot bands are collected in Table 3, along with the rotational constants determined by Guelachvili et al. [6] from their study of the C – H (ν_4) and C≡C (ν_5) stretching modes for comparison, whereas Table 4 presents the upper state constants for the $6_0^1 8_0^1$ band system.

The weak $5_0^1 6_0^1$, $1_0^1 9_0^1$, $1_0^1 9_1^0$, $1_0^1 8_1^0$ and $4_0^1 6_1^0$ perpendicular band systems were observed upon saturation of the ν_4 fundamental band of diacetylene during an experiment designed to record the spectrum of rare isotopomers in natural abundance. The lower and upper state rotational and distortion

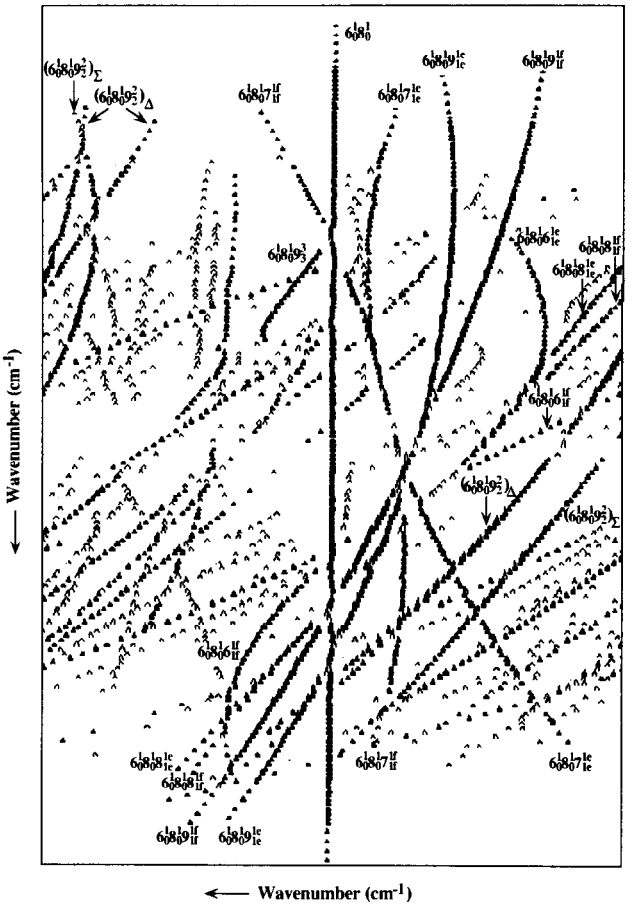

Fig. 2. A screen-dump of the Loomis–Wood diagram of the $6_0^1 8_0^1$ combination band of diacetylene.

constants and band origins for each cold band are listed in Table 5. It was not possible to assign any hot bands accompanying the combination and difference bands. The rotational assignments, observed transitions and deviations for the cold main bands of the $6_0^1 8_0^1$, $5_0^1 6_0^1$ and $1_0^1 9_0^1$ combination bands and the $1_0^1 9_1^0$, $1_0^1 8_1^0$, and $4_0^1 6_1^0$, difference bands, and a list of the hot bands associated with the $6_0^1 8_0^1$ combination band, are available as supplementary material[a].

[a] Deposited with B.L.L.D. as Supplementary Publication number SUP 26457 (22 pages).

TABLE 3

Rotational constants for diacetylene in various vibrational levels of the lower state of the $6_0^1 8_0^1$ combination band (cm^{-1})[a]

Level	Species	B''	$10^8 \times D''$	$10^4 \times q''$	$10^4 \times \alpha_i$	B''[b]	$10^8 \times D''$[b]	$10^4 \times q''$[b]	$10^4 \times \alpha_i$[b]	B''	$10^8 \times D''$
$6_0^1 8_0^1$	Σ_g^+	0.14641021(52)	1.6085(49)			0.14640981(51)	1.5569(48)			$0.1464109_6(11)$[c]	$1.565_9(10)$[c]
$6_0^1 8_0^1 9_{1e}^{1e}$	Π_u	0.14672627(70)	1.6628(82)	2.0397(92)	−3.1606(87)	0.14672644(68)	1.6068(77)	2.0422(93)	−3.1623(86)	$0.1467265_3(22)$[c]	$1.609_5(26)$[c]
$6_0^1 8_0^1 9_{1f}^{1f}$	Π_u	0.14693024(60)	1.6903(71)		−5.2003(79)	0.14693066(64)	1.6389(75)		−5.2045(82)	$0.1469308_2(21)$[c]	$1.639_4(26)$[c]
$6_0^1 8_0^1 9_{2e}^{2e}$	Σ_g^+	0.1472322(14)	3.478(28)		−8.220(14)	0.1472369(16)	3.508(39)		−8.267(16)	$0.1472439_3(19)$[c]	$3.810_8(88)$[c]
$6_0^1 8_0^1 9_{2e}^{2e}$	Δ_g	0.1472598(28)	0.147(49)		−8.496(59)					$0.1472499_8(31)$[c]	$-0.343_0(113)$[c]
$6_0^1 8_0^1 9_{2f}^{2f}$	Δ_g	0.14725402(98)	1.863(15)		−8.4381(110)	0.1472544(10)	1.819(19)		−8.442(10)	$0.1472499_3(11)$[c]	$1.693_3(32)$[c]
$6_0^1 8_0^1 9_3^3$	Π_u	0.1476673(40)	1.29(16)		−12.571(40)	0.1476563(18)	0.731(78)		−12.461(18)		
$6_0^1 8_0^1 8_{1e}^{1e}$	Π_u	0.1464285(22)	1.512(36)	0.762(37)	−0.183(22)	0.1464323(22)	1.569(37)	0.735(38)	−0.221(22)	0.14643455(8)[d]	$1.584_1(35)$[d]
$6_0^1 8_0^1 8_{1f}^{1f}$	Π_u	0.1465047(30)	1.206(97)		−0.945(30)	0.1465058(32)	1.24(10)		−0.956(35)	0.14651490(8)[d]	$1.584_1(35)$[d]
$6_0^1 8_0^1 7_{1e}^{1e}$	Π_g	0.1466177(14)	1.563(22)	1.238(22)	−2.075(14)	0.1466187(16)	1.519(26)	1.252(23)	−2.085(16)	$0.1466242_8(68)$[c]	$1.600_5(64)$[c]
$6_0^1 8_0^1 7_{1f}^{1f}$	Π_g	0.1467415(17)	1.674(34)		−3.313(17)	0.1467439(17)	1.667(35)		−3.337(17)	$0.1467287_2(58)$[c]	$1.513_4(73)$[c]
$6_0^1 8_0^1 6_{1e}^{1e}$	Π_g	0.1464408(14)	1.691(29)	0.798(19)	−0.306(14)	0.1464385(16)	1.598(38)	0.808(20)	−0.287(16)	0.14643749(7)[d]	$1.582_1(30)$[d]
$6_0^1 8_0^1 6_{1f}^{1f}$	Π_g	0.1465206(13)	1.627(25)		−1.104(13)	0.1465193(12)	1.570(26)		−1.091(12)	0.14652036(7)[d]	$1.582_1(30)$[d]
$6_0^1 8_0^1 9_{1f}^{1f} 8_{1f}^{1f}$	Σ_g^-	0.1470262(39)	1.00(14)		−6.160(39)	0.1470283(35)	1.56(12)		−6.181(35)		
$6_0^1 8_0^1 9_{1e}^{1e} 7_{1e}^{1e}$	Σ_u^+	0.1469382(52)	2.18(54)		−5.280(54)	0.1469354(71)	1.80(80)		−5.252(71)		
$6_0^1 8_0^1 9_{1f}^{1f} 6_{1f}^{1f}$	Σ_u^-	0.1470741(24)	2.270(78)		−6.639(24)	0.1470717(33)	2.06(11)		−6.615(33)		
$6_0^1 8_0^1 9_1^1 6_1^1$	Δ_u	0.1468995(42)	1.27(35)		−4.893(42)						

[a] Values in parentheses denote standard errors.
[b] Constants from ground state combination differences.
[c] Guelachvili et al. from ref. 6.
[d] Matsumura and Tanaka from ref. 15.

TABLE 4

Rotational constants for diacetylene in various excited vibrational states derived from the $6_0^1 8_0^1$ band (cm^{-1})

Level	Species	$\tilde{\nu}_0$	Q-branch	B'	$10^8 \times D'$	$10^4 \times q'$	B'^a	$10^8 \times D'^a$	$10^4 \times q'^a$
$6_0^1 8_0^1$	Σ_u^+	1241.060828(38)		0.14654767(52)	1.5606(49)		0.14654757(51)	1.6077(47)	
$6_0^1 8_0^1 9_{1e}^{1e}$	Π_g	1241.101938(55)	1241.10182	0.14685858(70)	1.6051(82)	2.0620(92)	0.14685850(66)	1.6628(77)	2.0634(94)
$6_0^1 8_0^1 9_{1f}^{1f}$	Π_g	1241.101785(48)		0.14706478(60)	1.6351(71)		0.14706484(66)	1.6901(81)	
$6_0^1 8_0^1 9_{2e}^{2e}$	Σ_u^+	1241.198636(76)		0.1473634(14)	3.352(27)		0.1473680(17)	3.622(41)	
$6_0^1 8_0^1 9_{2e}^{2e}$	Δ_u	1241.17178(18)	1241.17466	0.1473915(28)	0.121(48)				
$6_0^1 8_0^1 9_{2f}^{2f}$	Δ_u	1241.172627(55)		0.14738443(97)	1.803(16)		0.1473848(12)	1.882(20)	
$6_0^1 8_0^1 9_3^3$	Π_g	1241.26700(13)		0.1477989(42)	1.13(15)				
$6_0^1 8_0^1 8_{1e}^{1e}$	Π_g	1239.07575(15)	1239.07602	0.1465630(22)	1.509(37)	0.807(39)	0.1465657(19)	1.551(30)	0.774(39)
$6_0^1 8_0^1 8_{1f}^{1f}$	Π_g	1239.07541(18)		0.1466437(32)	1.226(89)		0.1466431(34)	1.18(11)	
$6_0^1 8_0^1 7_{1e}^{1e}$	Π_u	1242.263712(13)	1242.26507	0.1467636(14)	1.518(23)	1.069(22)	0.1467643(13)	1.565(22)	1.059(25)
$6_0^1 8_0^1 7_{1f}^{1f}$	Π_u	1242.264324(93)		0.1468705(17)	1.624(35)		0.1468702(21)	1.668(43)	
$6_0^1 8_0^1 6_{1e}^{1e}$	Π_g	1237.60683(12)	1237.60838	0.1465366(14)	1.660(28)	1.565(19)	0.1465338(17)	1.616(41)	1.583(21)
$6_0^1 8_0^1 6_{1f}^{1f}$	Π_g	1237.606434(95)		0.1466931(13)	1.592(25)		0.1466921(18)	1.572(40)	
$6_0^1 8_0^1 9_{1f}^{1f} 8_{1f}^{1f}$	Σ_u^-	1238.15428(20)		0.1471615(40)	1.50(13)		0.1471663(38)	1.19(13)	
$6_0^1 8_0^1 9_{1e}^{1e} 7_{1e}^{1e}$	Σ_g^+	1240.13405(13)		0.1470673(53)	2.07(50)		0.1470698(75)	2.31(91)	
$6_0^1 8_0^1 9_{1f}^{1f} 6_{1f}^{1f}$	Σ_g^-	1239.54136(11)		0.1472070(25)	2.20(73)		0.1471998(27)	1.95(98)	
$6_0^1 8_0^1 9_1^1 6_1^1$	Δ_g	1239.27843(12)	1239.27970	0.1470364(43)	1.10(31)		0.1470406(76)	1.57(58)	

[a] Determined from excited state combination differences fits.

TABLE 5

Lower state and upper state rotational and distortion constants, and band origins for weak combination bands and difference bands of diacetylene (cm^{-1})

Band	Type	$\tilde{\nu}_0$	B''	$10^8 \times D''$	B'	$10^8 \times D'$
$1_0^1 9_0^1$	$\Pi_u - \Sigma_g^+$	3551.56158(59)	0.1464245(61)	2.42(29)	0.1465136(59)	2.64(31)
$5_0^1 6_0^1$	$\Pi_u - \Sigma_g^+$	2643.32323(32)	0.1464367(63)	2.11(28)	0.1460658(60)	2.11(30)
$1_0^1 9_1^0$	$\Sigma_g^+ - \Pi_u$	3112.17692(26)	0.1467222(50)	1.50(21)	0.1461832(50)	1.60(21)
$4_0^1 6_1^0$	$\Sigma_u^+ - \Pi_g$	2708.16608(23)	0.1464447(36)	1.58(13)	0.1461974(38)	1.78(12)
$1_0^1 8_1^0$	$\Sigma_g^+ - \Pi_u$	2704.25893(18)	0.1464336(21)	1.568(42)	0.1461880(21)	1.570(44)

DISCUSSION

The $6_0^1 8_0^1$ combination band and associated hot bands

The cold band consists of simple *P*- and *R*-branches and appears from the Loomis–Wood plot to be unperturbed. The value of 0.14641021(52) cm^{-1} for B_0 is in excellent agreement with that of $0.1464109_6(11)$ cm^{-1} reported by Guelachvili et al. [6]. The results quoted in this work are to one standard deviation, whereas the error limits from ref. 6 are to three standard deviations.

The $6_0^1 8_0^1 9_1^1$, $6_0^1 8_0^1 9_2^2$ and $6_0^1 8_0^1 9_3^3$ hot bands arise from the C≡C – H bending mode, ν_9. The *l*-doubling for the $6_0^1 8_0^1 9_1^1$ hot band ($\Pi_g - \Pi_u$) was resolved from $J' = 2$. The value for the effective *l*-type doubling constant, q_9'', in the lower state was determined from the *e* and *f* components to be $2.0421(91) \times 10^{-4}$ cm^{-1}, which agrees well with the value of $2.046(33) \times 10^{-4}$ cm^{-1} published by Matsumura and Tanaka from their analysis of the difference band $\nu_8 - \nu_6$, which appears in the microwave region [15]. The vibration–rotation interaction constants were determined to be $-3.1663(68) \times 10^{-4}$ cm^{-1} for α_{9e} and $-5.2084(75) \times 10^{-4}$ cm^{-1} for α_{9f}, and are in excellent agreement with the values of $-3.159(20) \times 10^{-4}$ cm^{-1} and $-5.205(20) \times 10^{-4}$ cm^{-1} from ref. 6. The upper vibrational state of the $6_0^1 8_0^1 9_2^2$ hot band consists of Σ_u^+ and Δ_u substates, and that of the $6_0^1 8_0^1 9_3^3$ hot band consists of Π_g and Φ_g substates. The *l*-resonance for the $6_0^1 8_0^1 9_2^2$ ($l = \pm 2$) hot band, which appeared perturbed, was resolved from $J' = 28$ and was observed adjacent to the Σ_u^+ sub-band on the Loomis–Wood plot. The Π_g sub-band of the $6_0^1 8_0^1 9_3^3$ hot band was tentatively assigned to a band which showed no intensity alternation and which was found to be Coriolis perturbed in both *P*- and *R*-branches and centred around $J' = 20$–21. However, the nature of the perturbing level has not been conclusively established. The band origin and unperturbed rotational and distortion constants were obtained by the use of ground-state combination differences of the observed transitions including those perturbed in the least-squares analysis. The Φ_g

sub-band was not conclusively identified. From the expressions $B_0 - (2\alpha_9)$ and $B_0 - (3\alpha_9)$, the lower state rotational constants for the $\upsilon_9 = 2$ and $\upsilon_9 = 3$ levels were predicted to be 0.1472463 cm^{-1} and 0.1476644 cm^{-1}, respectively. These are in reasonable agreement with the derived B'' values of 0.1472569(28) cm^{-1} and 0.1476673(40) cm^{-1} determined for the $\upsilon_9 = 2$ and 3 levels listed in Table 3. In the final data fit for the Π_u sub-band, the rotationally perturbed transitions were excluded from the analysis which included a total of 57 transitions. The values obtained for B'' and D'' for the e sublevel of the $\Delta - \Delta$ sub-band is anomalous, although the rotational assignments are considered definite. These anomalies may be due to l-type resonance which cannot be treated using our approach. A plot of the band origins for the $6_0^1 8_0^1$, $6_0^1 8_0^1 9_1^1$, $6_0^1 8_0^1 9_2^2$, and $6_0^1 8_0^1 9_3^3$ bands against the vibrational quantum number υ revealed an almost linear dependence of the band origins.

The $6_0^1 8_0^1 6_1^1$, $6_0^1 8_0^1 7_1^1$ and $6_0^1 8_0^1 8_1^1$ hot bands were observed to be of similar intensity and each band was accompanied by a sharp unresolved Q-branch. The starting point was the unambiguous assignment of the $6_0^1 8_0^1 6_1^1$ hot band. Analyses of the hot band gave a value of $-7.05(19) \times 10^{-5}\,cm^{-1}$ and $0.798(19) \times 10^{-4}\,cm^{-1}$ for α_6 and q_6'', respectively. The value for the vibration–rotation constant agrees well with the value of $-7.27(20) \times 10^{-5}\,cm^{-1}$ reported by Matsumura et al. [16], although the value for the l-doubling constant is not in good agreement with their value of $0.824(6) \times 10^{-4}\,cm^{-1}$. The more intense of the above two remaining hot bands was the $6_0^1 8_0^1 7_1^1$ hot band, assigned on the basis of Boltzman distribution and of the positioning of an intense Q-branch near the band centre. The derived value of $-2.694(22) \times 10^{-4}\,cm^{-1}$ for α_7 from the least-squares analyses of the observed transitions, matches well the value of $-2.656(90) \times 10^{-4}\,cm^{-1}$ deduced from the work carried out by Guelachvili et al. [6]. However, the value of $1.238(22) \times 10^{-5}\,cm^{-1}$ for q_7'' is not a good match with their value of $1.045(89) \times 10^{-4}\,cm^{-1}$. The band centre and low J transitions in both P- and R-branches of the remaining intense doublet which was identified as the $6_0^1 8_0^1 8_1^1$ hot band, were masked in the spectrum by several of the close overlapping hot bands, as shown in the Loomis–Wood plot. A series of least-squares analyses was carried out for every possible set of rotational assignments and the band origin was determined on the basis of the best match between observed rotational and l-doubling constants with known values. As shown in Table 3, the average value for the vibration–rotation constant, α_8, from the $6_0^1 8_0^1 8_1^1$ hot band was determined to be $-5.93(41) \times 10^{-5}\,cm^{-1}$, which is in reasonable agreement with the value of $-6.83(20) \times 10^{-5}\,cm^{-1}$ from ref. 15. Similarly, the derived value for the l-doubling constant, q_8'', of $7.35(38) \times 10^{-5}\,cm^{-1}$ agrees poorly with their value of $8.030(12) \times 10^{-5}\,cm^{-1}$.

Several fragments of weak hot bands were observed, some of which

showed a definite intensity alternation and which may be attributed to the $6_0^1 8_0^1 9_1^1 7_1^1$, $6_0^1 8_0^1 9_1^1 6_1^1$, $6_0^1 8_0^1 9_1^1 8_1^1$ and $6_0^1 8_0^1 3_1^1$ hot bands. Of these, the $6_0^1 8_0^1 9_1^1 8_1^1$, $6_0^1 8_0^1 9_1^1 7_1^1$ and $6_0^1 8_0^1 9_1^1 6_1^1$ hot bands have been tentatively assigned. The former and latter two hot bands are composed of three components which are of the type $\Sigma_u^+ - \Sigma_g^+$, $\Sigma_u^- - \Sigma_g^-$ and $\Delta_u - \Delta_g$ and $\Sigma_g^+ - \Sigma_u^+$, $\Sigma_g^- - \Sigma_u^-$ and $\Delta_g - \Delta_u$, respectively. The expected rotational constants, B''_{av}, for the lower vibrational state were estimated from the expressions $B_0 - (\alpha_9 + \alpha_8)$, $B_0 - (\alpha_9 + \alpha_7)$ and $B_0 - (\alpha_9 + \alpha_6)$ to be 0.1468846 cm^{-1}, 0.1468988 cm^{-1} and 0.1470977 cm^{-1}, respectively. Least-squares analyses of the observed wavenumber values for the observed transitions yielded the results included in Tables 3 and 4.

The starting point for the analyses of these weak hot bands was the unequivocal assignment of the $6_0^1 8_0^1 9_1^1 6_1^1$ hot band of $\Delta_g - \Delta_u$ symmetry type. The localisation of a weak Q-branch assisted in the assignment. The e and f sublevels were not resolved, such that no intensity alternation was discernible along the P- and R-branches. The $6_0^1 8_0^1 9_{1f}^{1f} 6_{1f}^{1f}$ sub-band was observed adjacent to the $\Delta_g - \Delta_u$ sub-band. The derived value of 0.1470741(24) cm^{-1} for B'' is in good agreement with the expected value of 0.1470406 cm^{-1} for the f sublevel. The next hot band, observed with distinct intensity alternation, was tentatively assigned to the Σ_u^+ component of the $6_0^1 8_0^1 9_1^1 7_1^1$ hot band, on the basis of good agreement between the derived value of 0.1469382 cm^{-1} for B'' and the expected value of 0.1469399 cm^{-1} from the expression $B_0 - (\alpha_{9e} + \alpha_{7e})$. The remaining Σ_u^- and Δ_u sub-bands were not conclusively identified. Another band observed as a single series with weak and strong components was assigned to the Σ_g^- sub-band of the $6_0^1 8_0^1 9_1^1 8_1^1$ hot band. The determined value of 0.1470262(39) cm^{-1} agrees well with the expected value of 0.1470299 cm^{-1} estimated from $B_0 - (\alpha_{9f} + \alpha_{8f})$. Several other hot bands and fragments of branches were identified with the help of the MACLOOMIS program, but it has not been possible to conclusively make any assignments as no spectroscopic information could be derived from the least-squares analyses of the observed transitions of these bands.

The $5_0^1 6_0^1$ and $1_0^1 9_0^1$ combination bands, and $4_0^1 6_1^0$, $1_0^1 8_1^0$ and $1_0^1 9_1^0$ difference bands

The above bands were observed with weak P- and R-branches, discernible up to $J' = 40$ or 65 quantum number, and with relatively dense Q-branches. It was not possible to identify hot bands in any of the above band systems or assign the overlapping and congested Q-branches. The $5_0^1 6_0^1$ and $1_0^1 9_0^1$ combination bands, and $4_0^1 6_1^0$, $1_0^1 8_1^0$ and $1_0^1 9_1^0$ difference bands were rotationally assigned on the basis of the expected intensity alternation for even and odd J lines, and on the value of the lower or upper state rotational constants for the various vibrational levels which have been previously

determined in this work. Improved band origins for the ν_6, ν_8, ν_1 and ν_9 fundamental bands were obtained from the difference bands and from the use of the known value of $\nu_8 - \nu_6$ reported by Matsumura et al. [15]. The derived vibrational frequencies of greater accuracy have been included in Table 2.

STRUCTURE OF DIACETYLENE, TRIACETYLENE AND DICYANOACETYLENE

In order to obtain rotational constants for further isotopomers of diacetylene and so derive structural parameters, a measurement of the spectrum at pressures high enough to saturate the parent band was carried out to search for the ν_4 fundamental bands of the ^{13}C and ^{2}H isotopomers of diacetylene in natural abundance. Ab initio calculations predicted frequency shifts of 8 and 5 cm^{-1} for the $H-C\equiv{}^{13}C-C\equiv C-H$ and $H-{}^{13}C\equiv C-C\equiv C-H$ species, respectively. The high J transitions of the ^{13}C isotopomers are thought to have been observed, but it was impossible to establish conclusively the correct band centre due to overlapping with the strong parent band. The band due to the deuterated isotope $^{2}H-C\equiv C-C\equiv C-H$ at 2600 cm^{-1} [17] was not observed in our experiments. Consequently only a single rotational constant is available from which to ascertain structural parameters. Without the rotational constants of the other isotopomers, the best method for obtaining geometric information on diacetylene and similar symmetric acetylenic molecules is to use the single rotational constant together with the results of ab initio calculations, using appropriately large basis sets and estimates from similar molecules of known geometries. Although ab initio calculations predict r_e and B_e values, the results can be compared directly with r_0 and B_0 values derived from experiment, because for linear molecules with more than three atoms there is a tendency for the summation term in expression (2) to be very close to zero. This happens because the vibration–rotation parameters, α_i, are negative for the bending modes and positive for the stretching modes and, thus, the contributions tend to cancel each other in the summation. For example, for dichloroacetylene the difference between B_e and B_0 is less than 1×10^{-5} cm^{-1} [18].

Table 1 includes an estimated value for the rotational constant B_0 of diacetylene obtained by simply transferring the known bond lengths of the related molecule cyanoacetylene, HC_3N, into the equivalent bonds of diacetylene. This procedure results in an estimate of the B value to within 0.08% of the experimental B_0 value. This procedure has been used with some success for dicyanoacetylene [11] and triacetylene [7] with HC_5N as the model molecule, and the principal is similar to that used by Oka [19] for the successful prediction of the rotational constants of the experimentally unknown molecules HC_9N and $HC_{11}N$ prior to their detection in the inter-

stellar medium. The ab initio geometry optimization carried out at the Hartree–Fock level results in a much shorter bond length for the C≡C bond and, consequently, an overestimation of the *B* rotational constant. However, calculations carried out with the inclusion of electron correlation with second-order Moeller–Plesset theory overestimate the C≡C bond length and underestimate the *B* value. Ab initio calculations carried out on the related species NC_4N and HC_6H at the same levels of theory result in similar under- and overestimations as can be seen in Table 1. The results of calculations using MP3 and MP4 theory show similar trends for all molecules with no improvement in the prediction of bond lengths. For such simple linear systems of first row elements it might have been expected that as the theory is taken from HF/6-31G** through to MP4/6-31G** the predicted bond lengths would approach the equilibrium bond lengths. This does not seem to be the case. Similar sets of calculations were carried out on HC_3N and HC_5N, and the results in Table 1 again show the same trends with either the single bonds or the triple bonds overestimated and with the bond lengths bracketing, but not approaching the experimental values as the calculations are taken to higher orders of theory. Ab initio calculations carried out over the complete set of molecules give consistent results for all the parameters and so the use of scaling parameters results in an adequate set of bond lengths for the symmetric acetylene species that predict the experimental *B* values well. The estimates using bond lengths taken from HC_3N and HC_5N predict the *B* values as well as, or better than, the ab initio values. One reason for going to such lengths to ascertain the geometries of these species was that the r_0 geometry of dicyanoacetylene derived from electron diffraction data [13] appeared to be inconsistent with the value estimated in the infrared study of Winther et al. [11]. The present data confirm the conclusions of Winther et al. on the geometry of dicyanoacetylene, and the estimated geometries for diacetylene, triacetylene and dicyanoacetylene included in Table 1 would seem to be the most accurate structures available without recourse to the direct calculation of geometries using isotopic substitutions.

ACKNOWLEDGMENTS

This work was supported by an Australian Research Council grant. D.N.B. acknowledges the support of an Australian Commonwealth Postgraduate Studentship.

REFERENCES

1 V.G. Kunde, A.C. Aikin, R.A. Hanel, D.E. Jennings, W.C. Maguire and R.E. Samuelson, Nature, 292 (1981) 686–688.
2 A. Coustenis, B. Bézard and D. Gautier, Icarus, 80 (1981) 54–76.

3 P.N. Romani and S.K. Atreya, Icarus, 74 (1988) 424–445.
4 J.L. Hardwick, D.A. Ramsay, J.M. Garneau, J. Lavigne and A. Cabana, J. Mol. Spectrosc., 76 (1979) 492–505.
5 K. Matsumura, K. Kawaguchi, E. Hirota and T. Tanaka, J. Mol. Spectrosc., 118 (1986) 530–539.
6 G. Guelachvili, A.M. Craig and D.A. Ramsay, J. Mol. Spectrosc., 105 (1984) 156–192.
7 D. McNaughton and D.N. Bruget, J. Mol. Spectrosc., 150 (1991) 620–634.
8 G. Guelachvili and K. Narahari Rao, Handbook of Infrared Standards, Academic Press, New York, 1986.
9 D. McNaughton, D. McGilvery and F. Shanks, J. Mol. Spectrosc., 149 (1991) 458–473.
10 M.J. Frisch, M. Head-Gordon, H.B. Schlegel, K. Raghavachari, J.S. Binkley, C. Gonzalez, D.J. Defrees, D.J. Fox, R.A. Whiteside, R. Seeger, C.F. Melius, J. Baker, R.L. Martin, R.L. Kahn, J.J.P. Stewart, E.M. Fluder, S. Topiol and J.A. Pople, GAUSSIAN 88, Gaussian Inc., Pittsburgh, PA, 1988.
11 F. Winther, M. Schonhoff, A. Guarnieri, R. Le Prince, D. McNaughton and D.N. Bruget, J. Mol. Spectrosc., 152 (1992) 205–212.
12 A.J. Alexander, H.W. Kroto and D.R.M. Walton, J. Mol. Spectrosc., 62 (1976) 175–180.
13 K.W. Brown, J.W. Nibler, H. Hedberg and L. Hedberg, J. Phys. Chem., 93 (1889) 5679–5684.
14 R.A. Creswell, G. Winnewisser and M.C.L. Gerry, J. Mol. Spectrosc., 65 (1977) 420–429.
15 K. Matsumura and T. Tanaka, J. Mol. Spectrosc., 96 (1982) 219–233.
16 K. Matsumura, T. Etoh and T. Tanaka, J. Mol. Spectrosc., 96 (1981) 106–107.
17 N.L. Owen, C.H. Smith and G.A. Williams, J. Mol. Struct., 161 (1987) 33–53.
18 D. McNaughton, J. Struct. Chem., 3 (1992) in press.
19 T. Oka, J. Mol. Spectrosc., 72 (1978) 172–174.